

Broadened second excitonic transition of single-walled carbon nanotubes in photoluminescence excitation spectroscopy

Sebastian Heeg*, Benjamin Hatting, Marcus Dantz, and Stephanie Reich

Fachbereich Physik, Freie Universität Berlin, Arnimalle 14, 14195 Berlin, Germany

Received 18 June 2010, revised 3 August 2010, accepted 4 August 2010

Published online 13 September 2010

Keywords carbon nanotubes, excitation bandpass, excitonic transition, photoluminescence excitation

* Corresponding author: e-mail sebastian.heeg@physik.fu-berlin.de, Phone: +49 30 83856157, Fax: +49 30 83856081

In this paper, we investigate how photoluminescence excitation spectra of single-walled carbon nanotubes are influenced by experimental conditions. The use of incoherent light sources leads to a broadening of the second excitonic transition. We describe the broadening by a straight

forward simulation and deliver the width of the second excitonic transition free of experimental influences. A set of simulated data allows for the correction of experimental influences for arbitrary nanotubes chiralities and excitation bandpasses.

© 2010 WILEY-VCH Verlag GmbH & Co. KGaA, Weinheim

1 Introduction After the first observation of bandgap fluorescence from isolated single-walled carbon nanotubes [1] and successful assignment to (n,m) chiralities [2], photoluminescence spectroscopy has become a widely used tool in carbon nanotubes characterization [3]. Photoluminescence data are used, e.g., to tackle the abundance problem [4–8], to verify solubilization efficiencies of various surfactants [9, 10], as well as the efficiency of carbon nanotube separation techniques [11]. Photoluminescence excitation (PLE) in particular has its share in the investigation of electron–hole interactions [12].

In a PLE map, the excitation energy is plotted versus the luminescence. A peak in such a PLE map may correspond to the luminescence signal of a semiconducting nanotube of a certain chirality. Here the excitation resonantly matches the energy E_{22} of the second excitonic transition [13, 14] and the emission refers to the energy E_{11} of the first excitonic transition. A bandpass in excitation affects the width ΔE_{22} of the second transition. Some of us previously related the increase of ΔE_{22} with increasing excitation bandpass to broadened absorption due to deviations from Beer’s law of absorption and discussed the consequences for the interpretation of luminescence data [15].

In this paper, we review the correlation between the experimentally observed width of the E_{22} transition and the bandpass in excitation for a large range of parameters. A simulation allows for the determination of the intrinsic width

of E_{22} for a broad range of different bandpasses. By comparing the simulation with experimental data, we discuss the accuracy of a single-bandpass measurement. We present a set of simulated data, which enables the reader to estimate the intrinsic width of the E_{22} transition.

2 Experimental The sample investigated consisted of HiPCO tubes, which were solubilized using sodium dodecylbenzene sulfonate (SDBS) as surfactant after sonification. The measurements were carried out using an Horiba Yobin Ivon Fluorolog-3 Spectrofluorometer. The luminescence data were normalized with respect to the light source via dividing by the lamp intensity, which was measured using a Si-diode. The spectrometer response was normalized using a known reference source. The integration time was kept constant at 1 s and the bandpass in emission at 6 nm. The bandpass in excitation was varied between 4 and 14 nm. A PLE map recorded with an excitation bandpass of 10 nm is shown in Fig. 1.

A vertical cut at a fixed emission energy is called PLE spectrum. The PLE peaks were fitted using Lorentzian profiles associated with the resonant excitonic transition E_{22} and a constant background, which has been related to non-resonant continuum excitations [3]. The fitting is most accurate for smaller diameter tubes which are isolated energywise. With increasing diameter, the transition energies of the nanotubes are grouped and the fitting error increases.

© 2010 WILEY-VCH Verlag GmbH & Co. KGaA, Weinheim

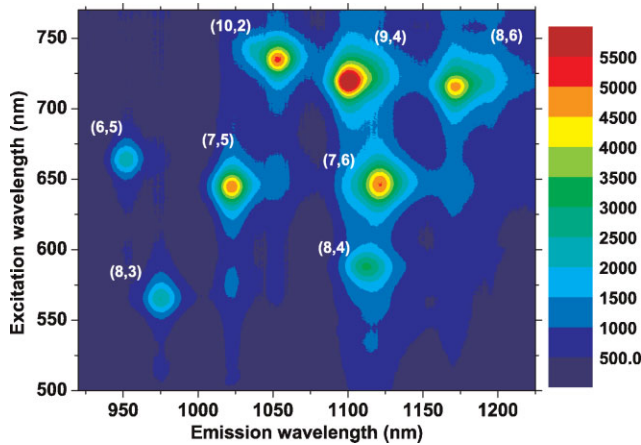


Figure 1 (online color at: www.pss-b.com) PLE map of the nanotubes species investigated. The photoluminescence peaks were assigned to chiralities in agreement with previous data [2]. The intensities (arb. units) are decoded by colors.

3 Excitation bandpass In Fig. 2, we depict the width of the E_{22} transition, ΔE_{22} , as full symbols for different nanotube species taken at various excitation bandpasses. For each of the nanotube species, the rightmost square¹ corresponds to an excitation bandpass of 14 nm. The bandpass was decreased in steps of 2 nm down to 4 nm. The width of the E_{22} transition decreases with decreasing experimental bandpass. As E_{22} varies with the chirality, every nanotube species is excited with a different energetic bandpass. The energetic width of a 14 nm bandpass may differ up to 25 meV between different chiralities for the

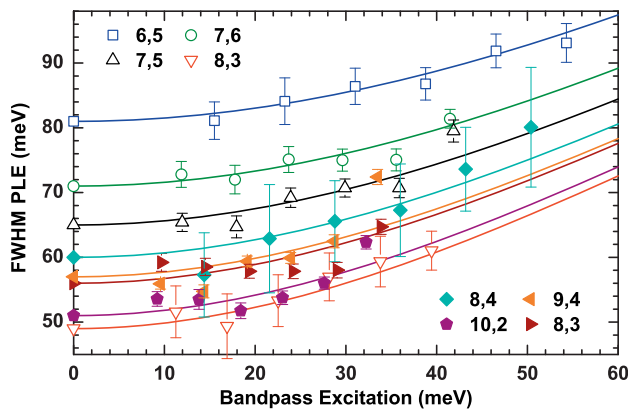


Figure 2 (online color at: www.pss-b.com) Measured width (symbols) and simulated data (lines) of the E_{22} transition versus excitation bandpass for different nanotube chiralities. The leftmost symbols indicate the extrapolated values for zero bandpass. The rightmost symbols indicate the 14 nm experimental bandpass and vary for different chiralities with E_{22} . Open symbols indicate data previously published by some of us [15].

¹ The leftmost symbols at zero bandpass do not correspond to experimental values. They are depicted in order to assign simulated values (lines) to the corresponding chiralities.

nanotubes investigated. The authors are not aware of photoluminescence data acquired with a bandpass of more than 10 nm. Nevertheless, it is necessary to take into account large bandpasses in order to understand the broadening of ΔE_{22} qualitatively and quantitatively.

We assume that a PLE spectrum can be interpreted as an absorption spectrum, where the measured luminescence serves as the detection channel. The energetic bandwidth of the excitation (8–55 meV) is the same order of magnitude as the width of the E_{22} transition. The absorption coefficient varies substantially within the bandwidth of the excitation and leads to averaged or broadened absorption. The absorption intensity decreases at the center of the absorption profile and increases at its tails, leading to an overall broadening of the absorption and – in our case – the PLE spectra. We simulate the averaging by integrating the absorption $A^i(E)$ over different excitation bandpasses [15]

$$A^i(E) = \frac{1}{\text{BP}_{\text{eV}}^i(E)} \int_{E-0.5\text{BP}_{\text{eV}}^i(E)}^{E+0.5\text{BP}_{\text{eV}}^i(E)} \frac{1}{1 + \left(\frac{E-E_{22}}{\Delta E_{22}/2}\right)^2} dE, \quad (1)$$

where E denotes the excitation energy and $\text{BP}_{\text{eV}}^i(E)$ the energetic width excitation bandpass. The superscript i refers to the bandpass specified in nanometers. ΔE_{22} represents the width of the second excitonic transition free of experimental influences which is equal to zero bandpass. It serves as the input parameter for the simulation. We obtain the corresponding values of ΔE_{22} for a non-zero bandpass by fitting the broadened absorption spectra given by Eq. (1) with Lorentzians.

The calculated values of ΔE_{22} for the corresponding nanotubes are plotted versus the bandpass as solid lines in Fig. 2. We found the optimal value for the E_{22} by the method of least squares with a precision of 1 meV. A very good agreement between experiment and simulation is found for chiralities which are isolated with respect to energy on a PLE map. We found a good agreement for nanotubes with larger diameters (full symbols in Fig. 2), whose transition energies overlap and reduce the fitting accuracy.

An additional source of uncertainty is caused by the inhomogeneous intensity distribution of the light source within the excitation bandpass. In the model for broadened absorption given in Eq. (1) we assume the lamp intensity to be constant for any chosen bandpass. This assumption only holds if the lamp intensity varies slowly with the wavelength. In Fig. 3a, we depict lamp spectra taken at different nanometer bandpasses. The vertical line slightly above 1.6 eV shows how the position of a specific lamp peak shifts with increasing bandpass due to averaging. In Fig. 3b, we plot the ratio of the lamp spectra shown in Fig. 3a relative to the one acquired with the smallest bandpass (6 nm). If the lamp intensities were constant within the chosen bandpass, we would expect the ratio to be constant. A deviation from the mean values indicates that the normalized PLE spectra are biased by the excitation bandpass.

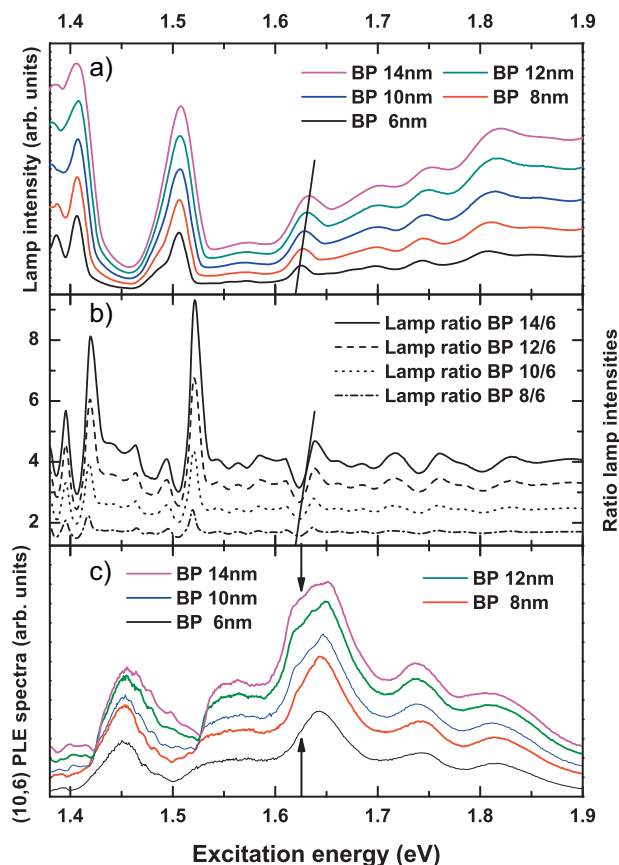


Figure 3 (online color at: www.pss-b.com) (a) Lamp spectra for different excitation bandpasses. Due to averaging, lamp peaks may shift towards higher lamp intensities as indicated by the vertical line. (b) Ratio of lamp spectra taken at different bandpasses. Deviations from the average values indicate high gradients in the lamp spectra. (c) PLE spectra of the (10,6) tube taken at different bandpasses. The averaging indicated by the vertical line as in (a) causes an unphysical peak, marked by arrows, to arise. PLE spectra have been acquired at an acquisition time of 10 s due to low luminescence intensity.

If a strong lamp gradient coincides with the E_{22} transition of a nanotube, the corresponding PLE peak becomes strongly biased by the lamp intensity normalization. This may lead to asymmetric, ill-shaped peaks whose center may be shifted. We demonstrate this for the (10,6) nanotube ($E_{22} \approx 1.64$ eV), whose normalized PLE spectra for different bandpasses are depicted in Fig. 3c. With increasing bandpass a side peak without any physical meaning starts to arise on the low energy side, indicated by the arrows in Fig. 3c. If the PLE data do not show a high gradient, however, the effects are small and remain unnoticed.

4 Results and discussion The simulated values for ΔE_{22} describe well the decrease of ΔE_{22} with decreasing excitation bandpass. The width of the second excitonic transition free of experimental parameters can only be obtained if the excitation bandpass is taken into consideration. We confirmed the model of broadened absorption given in Eq. (1) for nanotubes which are isolated with respect

to energy. For nanotubes of larger diameters, the fitting procedure becomes less accurate due to overlap with neighboring nanotube species, but the general behavior can be confirmed regarding those nanotubes as well.

In Fig. 4, we depicted simulated values of ΔE_{22} due to excitation bandpass broadening for a number of parameters. For intrinsic widths between 45 and 85 meV – indicated by the dashed lines – we verified the observed behavior with experimental values as depicted in Fig. 2. The data shown in Fig. 4 may help the reader to:

1. Evaluate how strongly PLE spectra are affected by broadening for an arbitrary combination of transition energy E_{22} and experimental bandpass.
2. Determine ΔE_{22} free of experimental influences for any given nanotube species as indicated by the authors in Fig. 2.
3. Decide whether the broadening affects the desired information obtained from luminescence data if different nanotube species are compared.
4. Evaluate the quality of the obtained parameters. If the fitting is not accurate or a PLE peak is biased by a strong lamp intensity gradient, the values for ΔE_{22} will deviate from the behavior shown.

As the broadening depends on E_{22} of the corresponding nanotube species, the width of the E_{22} transition – itself depending on the chirality – has to be considered for relative photoluminescence intensities. A detailed discussion can be found in Ref. [15].

In conclusion, we demonstrated how the second excitonic transition of semiconducting single-walled carbon

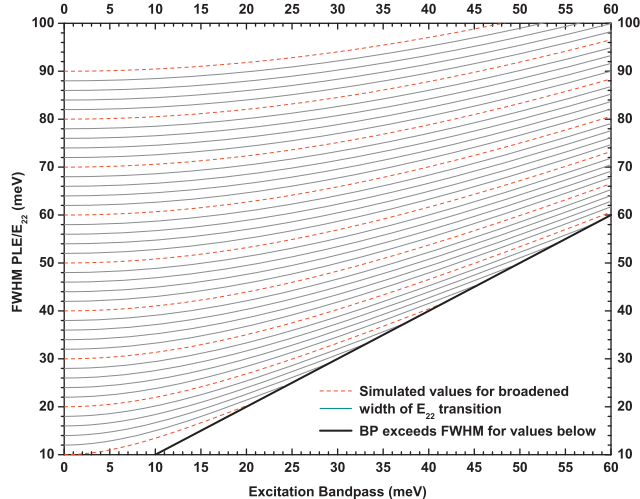


Figure 4 (online color at: www.pss-b.com) Simulated values for broadening of the second excitonic transition over excitation bandpass. Note that smaller intrinsic widths are more influenced by the bandpass. The values shown have been verified by measurements for intrinsic FWHMs between 45 and 85 meV. For values below the diagonal line, the bandpass exceeds the width of the luminescence excitation peaks.

nanotubes is broadened if broadband light sources are employed in photoluminescence spectroscopy. We related the broadening to variations of the absorption coefficient within the energetic bandwidth of the excitation radiation. At energies with high lamp intensity gradient, this gave rise to PLE features without physical meaning. These features could only be determined by the comparison of PL data acquired with different experimental bandpasses. A simulation delivered a tool to obtain the width of E_{22} . It may help the reader to improve the accuracy of PL data and to decide whether broadening affects the investigated properties or not.

Acknowledgements We thank Joel T. Abrahamson and Michael S. Strano for supply with CNT samples, and Heiko Dumlich for useful discussions and proof reading. We acknowledge funding by the ERC under grant number 210642.

References

- [1] M. O'Connell, S. Bachilo, C. Huffman, V. Moore, M. Strano, E. Haroz, K. Rialon, P. Boul, W. Noon, C. Kittrell, J. Ma, R. Hauge, R. Weisman, and R. Smalley, *Science* **297**(5581), 593–596 (2002).
- [2] S. M. Bachilo, M. S. Strano, C. Kittrell, R. Hauge, R. Smalley, and R. B. Weisman, *Science* **298**(5602), 2361–2366 (2002).
- [3] J. Lefebvre, S. Maruyama, and P. Finnie, *Top. Appl. Phys.* **111**, 287 (2008).
- [4] Y. Miyauchi, S. Chiashi, Y. Murakami, Y. Hayashida, and S. Maruyama, *Chem. Phys. Lett.* **387**(1–3), 198–203 (2004).
- [5] Y. Oyama, R. Saito, K. Sato, J. Jiang, G. Samsonidze, A. Gruneis, Y. Miyauchi, S. Maruyama, A. Jorio, G. Dresselhaus, and M. Dresselhaus, *Carbon* **44**(5), 873–879 (2006).
- [6] A. Jorio, C. Fantini, M. Pimenta, D. Heller, M. S. Strano, M. Dresselhaus, Y. Oyama, J. Jiang, and R. Saito, *Appl. Phys. Lett.* **88**(2), 023109 (2006).
- [7] T. Okazaki, T. Saito, K. Matsuura, S. Ohshima, M. Yumura, Y. Oyama, R. Saito, and S. Iijima, *Chem. Phys. Lett.* **420**(4–6), 286–290 (2006).
- [8] S. Heeg, E. Malić, C. Casiraghi, and S. Reich, *Phys. Status Solidi B* **246**(11–12), 2740–2743 (2009).
- [9] W. Wenseleers, I. Vlasov, E. Goovaerts, E. Obraztsova, A. Lobach, and A. Bouwen, *Adv. Funct. Mater.* **14**(11), 1105–1112 (2004).
- [10] A. Setaro, C. S. Popeney, B. Trappmann, V. Datsyuk, R. Haag, and S. Reich, *Chem. Phys. Lett.* **493**, 147–150 (2010).
- [11] M. Arnold, A. Green, J. Hulvat, S. Stupp, and M. Hersam, *Nature Nanotechnol.* **1**(1), 60–65 (2006).
- [12] Y. Miyauchi, H. Ajiki, and S. Maruyama, *Phys. Rev. B* **81**(12), 121415 (2010).
- [13] F. Wang, G. Dukovic, L. Brus, and T. F. Heinz, *Science* **308**(5723), 838–841 (2005).
- [14] J. Maultzsch, R. Pomraenke, S. Reich, E. Chang, D. Prezzi, A. Ruini, E. Molinari, M. S. Strano, C. Thomsen, and C. Lienau, *Phys. Rev. B* **72**(24), 241402 (2005).
- [15] S. Heeg, J. Abrahamson, M. Strano, and S. Reich, submitted.